



HAL
open science

A Three-step Decomposition Method for Solving the Minimum-Fuel Geostationary Station Keeping of Satellites Equipped with Electric Propulsion

Clément Gazzino, Denis Arzelier, Luca Cerri, Damiana Losa, Christophe Louembet, Christelle Pittet

► **To cite this version:**

Clément Gazzino, Denis Arzelier, Luca Cerri, Damiana Losa, Christophe Louembet, et al.. A Three-step Decomposition Method for Solving the Minimum-Fuel Geostationary Station Keeping of Satellites Equipped with Electric Propulsion. *Acta Astronautica*, 2019, 158, pp.12-22. 10.1016/j.actaastro.2018.08.015 . hal-01696455v2

HAL Id: hal-01696455

<https://laas.hal.science/hal-01696455v2>

Submitted on 19 Aug 2018

HAL is a multi-disciplinary open access archive for the deposit and dissemination of scientific research documents, whether they are published or not. The documents may come from teaching and research institutions in France or abroad, or from public or private research centers.

L'archive ouverte pluridisciplinaire **HAL**, est destinée au dépôt et à la diffusion de documents scientifiques de niveau recherche, publiés ou non, émanant des établissements d'enseignement et de recherche français ou étrangers, des laboratoires publics ou privés.

A Three-step Decomposition Method for Solving the Minimum-Fuel Geostationary Station Keeping of Satellites Equipped with Electric Propulsion

Clément Gazzino^a, Denis Arzelier^a, Luca Cerri^b, Damiana Losa^c, Christophe Louembet^a, Christelle Pittet^b

^aLAAS-CNRS, Université de Toulouse, CNRS, 7 avenue du Colonel Roche 31031 Toulouse, France

^bCNES, Centre Spatial de Toulouse, 18 Avenue Edouard Belin 31401 Toulouse, France

^cThales Alenia Space, 100 Bd du Midi 06156 Cannes la Bocca, France

Abstract

In this paper, a control scheme is elaborated in order to perform the station keeping of a geostationary satellite equipped with electric propulsion while minimizing the fuel consumption. The use of electric thrusters imposes to take into account some additional non linear and operational constraints that make the overall station keeping optimal control problem difficult to solve directly. That is why the station keeping problem is decomposed in three successive control problems. The first one consists in solving a classical optimal control problem with an indirect method initialized by a direct method without enforcing the thrusters operational constraints. Starting from this non feasible solution for the genuine problem, the thrusters operating constraints are incorporated in the second problem, whose solution produces a feasible but non optimal control profile via two different ways. Finally, the third optimizes the commutation times thanks to a method borrowed to the switched systems theory. Simulation results on a realistic example validate the benefit of this particular control scheme in the reduction of the fuel consumption for the geostationary station keeping problem.

Keywords: GEO Station Keeping, electric propulsion, fuel optimal control problem, Pontryagin Maximum Principle, Switched Systems Theory

1. Introduction

Due to orbital disturbing forces, any satellite in Geostationary Earth Orbit (GEO) drifts outside its station keeping (SK) window (a rectangular box of a given geographical longitude and latitude range). Performing an accurate SK strategy is therefore necessary to compensate for the induced environmental secular and periodic disturbances and to this end GEO spacecraft are equipped with electric and/or chemical thrusters.

Chemical propulsion systems have been and are still widely used. For these propulsion systems with high thrust capabilities, SK control laws are usually designed assuming an impulsive idealization of the thrust, as described for example in [1, 2, 3]. This type of propulsion is still used for the derivation of autonomous SK laws (see for instance the references [4, 5, 6, 7, 8]). The idea of using electric propulsion for station keeping dates back to the sixties. The references [9, 10, 11] describe generalities about the SK of a GEO satellite, and the reference [12] designs a control strategy in a simplified case. Some theoretical developments have then been conducted in the eighties. The reference [13] analyses the effect of electric North/South correction with constraints on the firing times while [14] model the secular evolution of the satellite and perform station keeping with a fixed number of thrusts. [15] derive a control strategy distinguishing short and long horizons. The patent [16] proposes a new configuration with four

thrusters mounted on the anti-nadir face of the satellite and derives a correction strategy while analyzing the effect of the orbital disturbances. This reference also describes the advantages (complete control of the three orbit vectors, remaining diagonal pair of thruster for a complete control in case of failure of one thruster) of this specific propulsion system based on HS 702 satellite with a xenon ion propulsion system. It has been widely used as a typical configuration for electric propulsion in the literature [17], [18], [19] and more recently [20]. Nowadays the electric propulsion is a viable alternative to the chemical one, in particular in the case of SK of GEO satellite ([21]), despite limiting thrust operations constraints (large on board power needs, mission requirements restricting the duration of use of the electric power system, impossibility to perform SK maneuvers at eclipse epochs, minimum elapsed time between two consecutive firing, on-off profile of the thrusters, thrust allocation). Indeed, the bigger specific impulse of electric thrusters leads to consequent savings in fuel consumption and a reduction of the satellite mass, enabling increased payload capacity and improved satellite lifetime.

Considering these technological and operational features, optimal control strategies for electric SK taking various constraints into account have to be carefully designed. The problem of fuel-optimal station keeping is in general expressed as an optimal control problem (OCP). Several types of techniques for solving the resulting optimal sta-

tion keeping control problem exist. When the thrust is considered as impulsive or when simple models are used to describe the disturbing forces, analytical solutions provide control laws, as in [22]. Otherwise, it is necessary to resort to numerical methods, such as direct collocation based methods as described in [23, 24, 25, 26, 27, 28]. For this family of approaches, the state and the control variables are discretized to transcribe the original optimal control problem into a non linear programming problem. Conversely, indirect methods rely on the derivation of necessary optimality conditions expressed via the so-called Pontryagin Maximum Principle (PMP) and on the numerical solution of the two-points boundary value problem obtained from these optimality conditions. In order to counteract uncertainties affecting the control law, the use of Model Predictive Control algorithms is proposed in [29, 30]. To deal with on-off models of thrusts, the references [31, 32] use the Pulse Width Modulation technique to generate rectangular profiles from a continuous one. [18] has formulated a method based on differential inclusion, and a first avenue for the use of decomposition methods to solve the problem is given in [19].

In the reference [33], the two first steps of a decomposition technique for solving the station keeping control problem is presented. For the first step, an indirect method based on the application of the PMP with mixed control-state constraints is applied to solve a simplified optimal SK control problem, without considering the hard constraints on the control law (thrust constraints such as latency between two bursts of the same thruster and no simultaneous thrusting for instance). In a second step, a numerical approach is used to enforce all the thrust constraints left apart at the first step, thanks to dedicated equivalence schemes. If the operational constraints are respected, the spacecraft trajectory is composed of thrusting arcs separated by coasting arcs. Thus, the control profile switches from a time interval where all thrusters are off to a time interval for which one thruster is on, and vice-versa. Therefore, the system can be viewed as a switched system composed by one subsystem per thruster and one subsystem describing the dynamics during coasting arcs. The reference [34] takes advantage of the method proposed by [35] consisting in computing the optimal switching times of switched systems thanks to a time change of coordinates. The idea of the proposed paper is hence to demonstrate the benefit of solving the station keeping problem with a three-step method. The two first steps are the ones of [33] and the third step optimizing the switching times between coasting arcs and actuated arcs highly improves the fuel consumption. Therefore, the proposed contribution describes the three-step decomposition method in a unified framework, allowing to illustrate the benefit of this three-step method on a real example given by our industrial partner and aerospace manufacturer Thales Alenia Space.

2. Problem statement

2.1. Geostationary Spacecraft Dynamics

The motion of a spacecraft orbiting the Earth on a Geostationary Earth Orbit (GEO) can be described with the equinoctial orbital elements as defined in [36]:

$$x_{eoe} = [a \quad e_x \quad e_y \quad i_x \quad i_y \quad \ell_{M\Theta}]^T \in \mathbb{R}^6, \quad (1)$$

where a is the semi-major axis, (e_x, e_y) the eccentricity vector, (i_x, i_y) the inclination vector, $\ell_{M\Theta} = \omega + \Omega + M - \Theta$ the mean longitude with Ω the right ascension of the ascending node, ω the perigee's argument, M the mean anomaly and $\Theta(t)$ the right ascension of the Greenwich meridian. The dynamics of the spacecraft may be represented by the following non linear state-space model:

$$\frac{dx_{eoe}}{dt} = f_L(x_{eoe}, t) + f_G(x_{eoe}, t)u. \quad (2)$$

$f_L \in \mathbb{R}^6$ is the Lagrange contribution part of the external disturbing forces. For a GEO spacecraft, the main disturbing forces are the non-spherical part of the Earth gravitational potential that mainly affects the mean longitude $\ell_{M\Theta}$, the solar radiation pressure (SRP) that mainly affects the eccentricity vector (e_x, e_y) and the gravitational attraction of the sun and the moon that mainly affects the inclination vector (i_x, i_y) (see [37]). These forces are described in detail by the CNES ORANGE model (cf.[38]) or in the reference [2]. $f_G \in \mathbb{R}^{6 \times 3}$ is the Gauss contribution part for the disturbing forces that do not derive from a potential. In the case of a GEO spacecraft, this contribution consists in the acceleration produced by the thrusters that can be viewed as a disturbing one.

$u = [u_R \quad u_T \quad u_N]^T \in \mathbb{R}^3$ is the control vector expressed in the local orbital RTN frame (also written RSW) defined in [2] by (see Figure 1):

- N is the unit vector along the kinetic momentum;
- R is the unit vector along the direction Earth's center - satellite;
- T completes the right-handed orthogonal direct basis.

In order to deal with the station keeping problem, the station keeping point is defined as:

$$x_{sk} = [a_{sk} \quad 0 \quad 0 \quad 0 \quad 0 \quad \ell_{M\Theta_{sk}}]^T \quad (3)$$

where a_{sk} is the geosynchronous semi-major axis and $\ell_{M\Theta_{sk}}$ is the station mean longitude.

The relative dynamics equations are developed by linearization of Equation (2) at the station keeping point (3) evolving on an ideal circular geostationary keplerian orbit. By denoting $x = x_{eoe} - x_{sk}$, the relative state model for the SK problem reads:

$$\frac{dx}{dt} = A(t)x + D(t) + B(t)u, \quad (4)$$

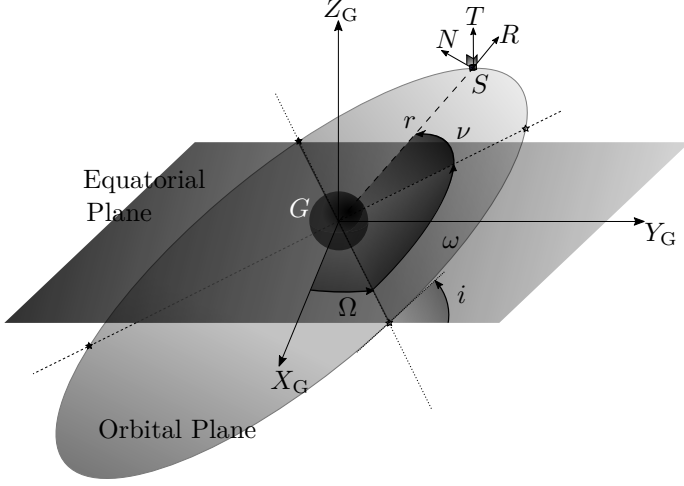


Figure 1: Geocentric inertial reference frame (G, X_G, Y_G, Z_G) and local orbital frame (S, R, T, N) .

where the matrices $A \in \mathbb{R}^{6 \times 6}$, $B \in \mathbb{R}^{6 \times 3}$, $C \in \mathbb{R}^{3 \times 6}$ and $D \in \mathbb{R}^6$ are defined as follows:

$$A(t) = \left. \frac{\partial}{\partial x_{eoe}} (f_L(x_{eoe}(t), t)) \right|_{x_{eoe}=x_{sk}}, \quad (5)$$

$$B(t) = f_G(x_{sk}, t), \quad (6)$$

$$D(t) = f_L(x_{sk}, t). \quad (7)$$

The geographical coordinates of the satellite:

$$y_{eoe} = T(x_{eoe}, t)x_{eoe}, \quad (8)$$

are of interest because the station keeping problem consists in constraining them in the vicinity of the station keeping geographical position $y_{sk} = [r_{sk} \ 0 \ \lambda_{sk}]^t$ where r_{sk} is the geosynchronous radius and λ_{sk} is the station keeping geographical longitude. The relative geographical position with respect to the station-keeping position is denoted by:

$$y = y_{eoe} - y_{sk} = T(x_{sk}, t)x = C(t)x, \quad (9)$$

and is obtained by linearizing Equation (8) with respect to the station keeping geographical position.

After the linearization, the station keeping requirements on the latitude and the longitude of the spacecraft are expressed by constraining the relative geographical position with respect to the centre of the SK window: $\forall t \in [t_0, t_f]$,

$$\left| [0 \ 1 \ 0]C(t)x(t) \right| \leq \delta \text{ and } \left| [0 \ 0 \ 1]C(t)x(t) \right| \leq \delta, \quad (10)$$

with δ being the half width of the SK window in the latitude and longitude directions and $[t_0, t_f]$ the optimisation horizon. A trajectory satisfying the SK constraints (10) is called a SK-feasible trajectory (see Figure 2).

2.2. Electric Propulsion System

The considered satellite is equipped with four electric thrusters mounted on the anti-nadir face, each of them

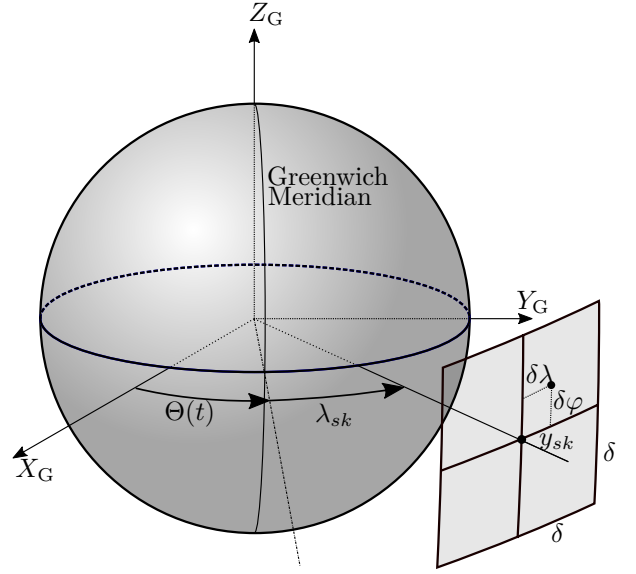


Figure 2: Station Keeping window.

having an orientation defined by a cant angle θ and a slew angle α . These angles define the North-East, the South-East, the North-West and the South-West directions of thrust. The satellite dynamics can be stated considering the four thrusts provided by the four engines as control variables. The control $u(t)$ expressed in the local orbital frame is a linear combination of the four thrusts such that $u = \Gamma F$, where $\Gamma = [\Gamma_1 \mid \Gamma_2 \mid \Gamma_3 \mid \Gamma_4] \in \mathbb{R}^{3 \times 4}$ and $F = [F_1 \ F_2 \ F_3 \ F_4]^T \in [0, F_{max}]^4$. The thrust direction vectors $\Gamma_j \in \mathbb{R}^3$ are given by:

$$\Gamma_j = \frac{1}{m} [-\sin \theta_j \cos \alpha_j \quad -\sin \theta_j \sin \alpha_j \quad -\cos \theta_j]^T, \quad (11)$$

where the cant angles θ_j and slew angles α_j are defined exactly as in [16] (see Figure 3). The mass m of the spacecraft is supposed to be constant.

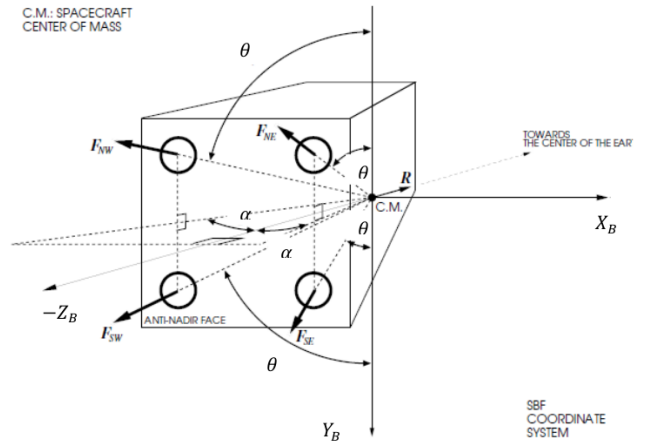


Figure 3: Orientation of the four thrusters (picture from TAS).

For the sake of simplicity, the thrust vector is normalized by the maximum level of thrust F_{max} . It is thus possible to write $F = F_{max} \tilde{F}$ with $\tilde{F} \in [0, 1]^4$. As the thrust profile is made of a series of on-off thrusts, the rectangular signal of the j^{th} thrust of the thruster i is parametrized by the date $t_{i,j}$ corresponding to the middle instant of the thrust and by its half width duration denoted $\Delta t_{i,j}$ (see Figure 4). The control function is thus rewritten as:

$$\begin{aligned} \tilde{F}(t) &= \tilde{F} \left(t, \{t_j^i, \Delta t_j^i\}_{\substack{i=1,\dots,4 \\ j=1,\dots,P_i}} \right), \\ &= \begin{bmatrix} \sum_{j=1}^{P_1} \mathbb{1}_{[t_j^1 - \Delta t_j^1, t_j^1 + \Delta t_j^1]}(t) \\ \sum_{j=1}^{P_2} \mathbb{1}_{[t_j^2 - \Delta t_j^2, t_j^2 + \Delta t_j^2]}(t) \\ \sum_{j=1}^{P_3} \mathbb{1}_{[t_j^3 - \Delta t_j^3, t_j^3 + \Delta t_j^3]}(t) \\ \sum_{j=1}^{P_4} \mathbb{1}_{[t_j^4 - \Delta t_j^4, t_j^4 + \Delta t_j^4]}(t) \end{bmatrix}. \end{aligned} \quad (12)$$

where P_i is the number of thrusts of thruster i .

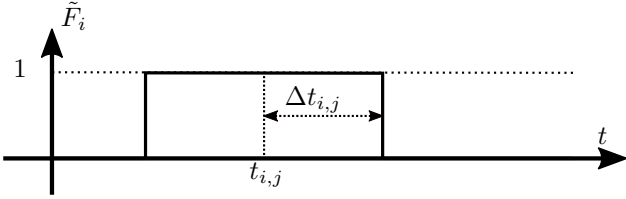


Figure 4: Parametrization of the j^{th} thrust of the thruster i .

Technological operational constraints inherent to the proposed actuation system are defined by:

- (i) thrusters cannot have simultaneous thrusts;
- (ii) a thrust must last at least $T_l : 2\Delta t_{i,j} \geq T_l$;
- (iii) two successive thrusts of a given thruster must be separated by an interval of latency equal to T_s ;
- (iv) two thrusts of two different thrusters must be separated by an interval of latency equal to T_d .

The restricted power available on-board prevents two thrusters from being active simultaneously and the minimum time latency between two thruster firings is imposed in order to allow an efficient battery recharge (see [19]).

The constraint for the time latency between the thrust k of thruster i and the thrust l of thruster j is mathematically expressed as:

$$|t_{i,k} - t_{j,l}| - (\Delta t_{i,k} + \Delta t_{j,l}) \geq K_{i,j}, \quad (13)$$

for $k = 1 \dots P_i$ and $l = 1 \dots P_j$, where $K_{i,j} = T_s$ if $i = j$ (constraint (iii)) and $K_{i,j} = T_d$ otherwise (constraint (iv)). In addition, some other convenient constraints force

the thrusters to be active only during the resolution time interval:

$$t_{i,j} - \Delta t_{i,j} \geq t_0 \quad \text{and} \quad t_{i,j} + \Delta t_{i,j} \leq t_f. \quad (14)$$

A trajectory satisfying the operational constraints for the considered electric propulsion system is called operationally feasible.

2.3. Fuel-optimal Station Keeping Control Problem

The main goal of the station keeping system is to maintain the longitude and the latitude of the satellite in a box defined by its size δ by acting on the orbital parameters via the 4 thrusters while reducing the fuel consumption to extend the operational lifetime of the satellite. The associated optimal control problem is in general defined over a fixed horizon for the computation of optimal control laws. The performance index to minimize in a Station Keeping operation is naturally defined as:

$$J = \int_{t_0}^{t_f} \sum_{\text{thruster } i=1}^4 \sum_{j=1}^{P_i} (|u_{R_{i,j}}(t)| + |u_{T_{i,j}}(t)| + |u_{N_{i,j}}(t)|) dt \quad (15)$$

$$= F_{max} \int_{t_0}^{t_f} \sum_{\text{thruster } i=1}^4 \|\Gamma_i\|_1 \sum_{j=1}^{P_i} |\tilde{F}_{i,j}(t)| dt \quad (16)$$

$$= 2F_{max} \sum_{\text{thruster } i=1}^4 \|\Gamma_i\|_1 \sum_{j=1}^{P_i} \Delta t_{i,j}. \quad (17)$$

Removing the constant multiplicative terms that does not affect the optimal solution, the objective function may be reduced to:

$$\tilde{J} = \sum_{i=1}^4 \sum_{j=1}^{P_i} \Delta t_{i,j}. \quad (18)$$

Considering all the constraints described above, the minimum-fuel SK problem to solve may be summarized as the following optimal control problem:

Problem 1. Find the sequence of dates $\{t_{i,j}\}$ and durations $\{\Delta t_{i,j}\}$, for $i = 1 \dots 4$, $j = 1 \dots P_i$ solutions of the minimization problem:

$$\begin{aligned} \min_{t_{i,j}, \Delta t_{i,j}} \tilde{J} &= \sum_{i=1}^4 \sum_{j=1}^{P_i} \Delta t_{i,j}, \\ \text{s.t.} \quad &\begin{cases} \dot{x}(t) = A(t)x(t) + D(t) \\ \quad + \tilde{B}(t)\tilde{F} \left(t, \{t_j^i, \Delta t_j^i\}_{\substack{i=1,\dots,4 \\ j=1,\dots,P_i}} \right), \\ x(t_0) = 0, \\ |[0 \ 1 \ 0]C(t)x(t)| \leq \delta, \quad |[0 \ 0 \ 1]C(t)x(t)| \leq \delta, \\ 2\Delta t_{i,j} \geq T_l, \quad t_{i,j} - \Delta t_{i,j} \geq t_0, \quad t_{i,j} + \Delta t_{i,j} \leq t_f, \\ |t_{i,k} - t_{j,l}| - (\Delta t_{i,k} + \Delta t_{j,l}) \geq K_{i,j}, \end{cases} \end{aligned} \quad (19)$$

with $\tilde{B}(t) = F_{max}\Gamma B(t)$. \circ

The Problem 1 raises some difficult mathematical issues. Firstly, due to the parametrization of the rectangular functions by $t_{i,j}$ and $\Delta t_{i,j}$, the dynamics define transcendental equations to be satisfied for the problem to solve. Secondly, the state constraints and the logical actuation constraints make the previous optimal control problem difficult to handle with existing methods. In addition, if the optimal number of thrusts per thruster is not known a priori, the problem to solve is a very challenging nonlinear mixed integer programming problem. For all these reasons, traditional solvers often fail to find a solution to the Problem 1.

The proposed paper aims thus at finding an efficient way to solve the fuel optimal station keeping problem by splitting the overall problem in a sequence of subproblems. The proposed resolution method consists in three different steps:

- (A) The thrusters constraints (13) and (14) are removed so that only an optimal control problem (OCP) with state and control constraints remains. This particular OCP is tackled via a hybrid approach relying on an indirect method initialized by a direct method solution dedicated to the search of adjoint variables as described in [39] and [40]. The PMP is applied to derive the first order necessary optimality conditions and the associated Two Points Boundary Value Problem (TP-BVP). This TPBVP is then solved via a collocation method. In order to recover an on-off profile from the continuous solution obtained, a threshold parameter $\varsigma = [\varsigma_1 \ \varsigma_2 \ \varsigma_3 \ \varsigma_4] \in \mathbb{R}^4$ has to be chosen. At the end of this step, the state trajectory fulfills the SK requirements but may not be operationally feasible.
- (B) As the result of the first step produces a control law that does not necessarily respect the thruster operational constraints, a second part is needed in order to obtain modified solutions compatible with actuation constraints (i)-(iv) and (14). The resulting state trajectory is operationally feasible but not necessarily SK-feasible.
- (C) The solution of step (B) being very sensitive to the threshold parameter ς chosen at step (A) the proposed third part optimizes the switching times for each thruster with the objective to reduce the fuel consumption. This step is based on an optimization technique stemming from the switched systems theory (see [35]) and takes advantage of the decomposition of the overall systems into several subsystems: one for each thruster being on and one when all the thrusters are off. The ensuing trajectory is both operationally and SK-feasible.

To sum up, instead of solving the overall SK problem at once, this problem is split into three smaller and simpler subproblems that are easier to solved in general. Section 3 will be devoted to the first part described above: solution of the simplified OCP via the hybrid method. Then

in Section 4, the thrusters constraints are enforced via the resolution of a second minimization problem called equivalence scheme. In Section 5, the switching times for each thrust are optimized using the switched systems theory, noticing that a system with a bang-bang control profile can be considered as being made up of two subsystems switching from one with control on to one with control off, and vice-versa. A commutation between a coasting arc and a fired arc is therefore interpreted as a commutation between the two subsystems.

3. Solution of the simplified OCP (step (A))

Removing the operational actuation constraints (13) and (14) allows to simplify the original optimal control problem. In particular, the thrust functions \tilde{F}_i are not modeled a priori as rectangular functions parametrized by $t_{i,j}$ and $\Delta t_{i,j}$ and the simplified OCP to be solved reads as :

Problem 2. Find the functions $t \mapsto \tilde{F}_i(t)$, $i = 1, \dots, 4$, solutions of the minimisation problem:

$$\min_{\tilde{F}(t) \in [0;1]^4} \tilde{J} = \int_{t_0}^{t_f} \sum_{i=1}^4 \tilde{F}_i(t) dt, \quad (20)$$

with the constraints:

$$\begin{cases} \dot{x}(t) = A(t) x(t) + D(t) + \tilde{B}(t) \tilde{F}(t), \\ |[0 \ 1 \ 0]C(t)x(t)| \leq \delta, \quad |[0 \ 0 \ 1]C(t)x(t)| \leq \delta, \\ x(t_0) = 0, x(t_f) = 0, \end{cases} \quad (21)$$

◦

Note that the constraint on the final state vector is not strictly necessary here from a theoretical point of view. However, this additional constraint may be heuristically justified by the numerous numerical experiments for which it proved to be helpful in reducing the sensitivity of the solution of Step A with respect to tuning parameters by preventing the longitude to end up on the boundary of the SK window.

Problem 2 is a minimum-fuel linear OCP defined on a fixed horizon with constraints both on the state and the control vectors. This problem is solved with the PMP.

The state geographical constraints are handled through the following additional state variable whose dynamics is given by (see the reference [41] for instance):

$$\dot{x}_7(t) = \psi(t, x(t)) = \sum_{i=1}^4 \frac{1}{2} \psi_i^2 \left[1 + \text{sign}(\psi_i(t, x(t))) \right], \quad (22)$$

with :

$$\psi_1(t, x(t)) = C_2(t)x(t) - \delta, \quad (23a)$$

$$\psi_2(t, x(t)) = -C_2(t)x(t) - \delta, \quad (23b)$$

$$\psi_3(t, x(t)) = C_3(t)x(t) - \delta, \quad (23c)$$

$$\psi_4(t, x(t)) = -C_3(t)x(t) - \delta, \quad (23d)$$

where $C_l(t)$ is the l^{th} line of the matrix $C(t)$.

The Hamiltonian of the system is:

$$\mathcal{H}(x(t), \tilde{F}(t), \lambda(t)) = \sum_{i=1}^4 \tilde{F}_i(t) + \mu_1 \psi(x(t)) + \lambda(t)^T [A(t)x(t) + D(t) + \tilde{B}(t)\tilde{F}(t)], \quad (24)$$

where $\lambda(t) \in \mathbb{R}^6$ is the adjoint vector, and μ_1 is a constant parameter. Choosing the value of this parameter allows to give more importance for minimizing the fuel consumption or enforcing of the SK constraints.

Applying the PMP described in [42] and [41], the minimization condition:

$$\mathcal{H}(x^*(t), \tilde{F}^*(t), \lambda^*(t)) = \min_{u \in [0,1]^4} \mathcal{H}(x^*(t), u(t), \lambda^*(t)) \quad (25)$$

leads to the following first order necessary switching condition for the optimal control:

$$\forall i = 1, \dots, 4, \tilde{F}_i^*(t) = \begin{cases} 1 & \text{if } 1 + [\lambda^{*T}(t)\tilde{B}(t)]_i < 0, \\ 0 & \text{if } 1 + [\lambda^{*T}(t)\tilde{B}(t)]_i > 0, \end{cases} \quad (26)$$

where $[h]_i$ stands for the i^{th} component of a generic vector h . The previous necessary condition can be rewritten using the switching function:

$$v \mapsto f_s(v) = \frac{1}{2} [(1 - \text{sign } v_1) \dots (1 - \text{sign } v_4)]^T, \quad (27)$$

leading to the optimal control:

$$\tilde{F}^*(t) = f_s(\mathbf{1} + \lambda^T(t)\tilde{B}(t)), \quad (28)$$

where $\mathbf{1}$ is a vector of ones.

The switching function:

$$f_s(\mathbf{1} + \lambda^T \tilde{B}) = \frac{1}{2} [\mathbf{1} - \text{sign}(\mathbf{1} + \lambda^T(t)\tilde{B}(t))] \quad (29)$$

defines a non continuous piecewise constant control profile. As the TPBV Problem 3 is solved with the *bvp4c* function of Matlab that requires continuous functions, the method described by [43] is used in order to approximate the discontinuous control profile into a continuous one. f_s is thus approximated by:

$$f_s(v) \approx \tilde{f}_s(v, M) = 1 - \frac{1}{\pi} \left[\arctan(Mv) + \frac{\pi}{2} \right], \quad (30)$$

where M is a parameter controlling the slope of the approximating switching function.

The two-point boundary value problem is built from the canonical equations of Hamilton and the transversality conditions and is defined as Problem 3

Problem 3. Find the functions x and λ solutions of the minimization problem:

$$\begin{aligned} \dot{x}(t) &= A(t)x(t) + D(t) + \tilde{B}(t)\tilde{f}_s(\mathbf{1} + \lambda^T \tilde{B}, M), \\ \dot{\lambda}(t) &= -A(t)^T \lambda(t) - \mu_1 \frac{d\psi}{dx}(x(t)), \\ x(t_0) &= 0, \quad x(t_f) = 0, \quad \lambda(t_0) \text{ and } \lambda(t_f) \text{ free.} \end{aligned} \quad (31)$$

o

This TPBVP is initialized by a direct collocation method, as described in the references [44] and [45] for instance, and then solved with an homotopy method in order to gradually increase the slope of the switching function by increasing accordingly the value of the parameter M of the approximated switching function.

A threshold parameter $\varsigma = [\varsigma_1 \ \varsigma_2 \ \varsigma_3 \ \varsigma_4]^T \in \mathbb{R}^4$ transforms the continuous profile into a discontinuous one as the Figure 5 shows. The decision variables, the middle times of the thrusts and their half-width durations are recovered. This transformation permits to extract from the on-off profile the number of thrusts for each thrusters P_i , $i = 1, \dots, 4$. According to Figure 5, it is clear that the value of the parameter ς has a direct influence on the associated half width thrust duration.

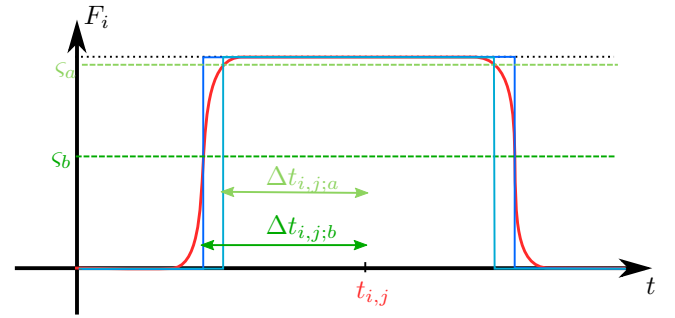


Figure 5: Effect of the threshold parameter ς on the half-width duration of the thrusts.

As the solution of Problem 3 does not satisfy in general the operational actuation constraints described in Section 2.2, the next section proposes an additional step for which an auxiliary problem enforces the actuation constraints on a new and equivalent control law, while preserving the structure and the overall effect of the thrust.

4. Enforcing the operational thrusters constraints (step (B))

The solution of the TPBV Problem 2 consists in a series of rectangle signals naturally resulting from the application of the PMP. However, this control law does not respect the actuation constraints left apart in the step (A). For instance, simultaneous activation of two different thrusters may occur. The aim of this second part is to find an equivalent control law ensuring that the resulting trajectory will be operationally feasible. Two different notions of equivalent control laws will be used hereafter.

The first notion of equivalence between two control laws relies on the fuel consumption argument: the goal is to compute a raw control profile that has the same fuel consumption as the profile obtained by solving the TPBV problem. Let \tilde{F}_{BVP} be the control obtained by solving Problem 3. Finding a Consumption Based Equivalent (CBE) control for the satellite is then equivalent to solve Problem 4 defined as follows:

Problem 4. Find the $t_{i,j}$ and the $\Delta t_{i,j}$, $i = 1, \dots, 4$, $j = 1, \dots, P_i$ minimising:

$$\min_{t_{i,j}, \Delta t_{i,j}} \sum_{i=1}^4 \left\| \tilde{F}_{\text{BVP},i}(t) \right\|_1 - 2 \sum_{j=1}^{P_i} \Delta t_{i,j}, \quad (32)$$

subject to the constraints:

$$\begin{cases} 2\Delta t_{i,j} \geq T_l, \\ |t_{i,k} - t_{j,l}| - (\Delta t_{i,k} + \Delta t_{j,l}) \geq K_{i,j}, \\ t_{i,j} - \Delta t_{i,j} \geq 0, \quad t_{i,j} + \Delta t_{i,j} \leq T. \end{cases} \quad (33)$$

◦

This problem is a non linear optimization problem where $\|\tilde{F}_{\text{BVP},i}(t)\|_1$ is the L^1 norm of the i^{th} component of the solution of Problem 3.

The second way to obtain an equivalent control respecting the actuation constraints is to define an "effect-based" equivalent (EBE) control. As the dynamics equation is given by Equation (4), the state vector at time t is given by:

$$x(t) = \Phi(t, t_0)x(t_0) + \int_{t_0}^t \Phi(t, \tau) [D(\tau) + B(\tau)\Gamma u(\tau)] d\tau, \quad (34)$$

where $\Phi(t, t_0)$ is the state transition matrix, implicitly defined by the homogeneous differential equation $\dot{\Phi}(t, t_0) = A(t)\Phi(t, t_0)$, $\Phi(t_0, t_0) = Id$ (see [46]).

To get a control profile that has the same effect at time t_f as the solution of Problem 3 and that respects the actuation constraints, the Problem 5 defined as follows has to be solved:

Problem 5.

$$\min_{t_{i,j}, \Delta t_{i,j}} \sum_{i=1}^6 \left[\int_{t_0}^{t_f} [\Phi(T, \tau) \tilde{B}(\tau) \tilde{F}_{\text{BVP}}(\tau)]_i d\tau - \sum_{k=1}^4 \sum_{j=1}^{P_k} \Delta t_{k,j} \int_{t_{k,j} - \Delta t_{k,j}}^{t_{k,j} + \Delta t_{k,j}} [\Phi(T, \tau) \tilde{B}(\tau)]_i d\tau \right]^2, \quad (35)$$

such that the constraints (33) are satisfied. ◦

Both Problems 4 and 5 can be solved by classical non linear optimization solvers.

The state trajectories obtained from the control profiles solutions of Problems 4 and 5 are very sensitive to the threshold parameter ς chosen at the end of the step (A). For some values of ς , the computing trajectory may be operationally feasible but not restricted to the SK window. The benefit of the step (B) is to provide a sequence of thrusting/coasting arcs admissible for the operational constraints (i)-(iv). This sequence is described by $\{U\} = \{U_1, \dots, U_K\}$, with:

$$U_k \in \left\{ \begin{bmatrix} 0 \\ 0 \\ 0 \\ 0 \end{bmatrix}, \begin{bmatrix} 1 \\ 0 \\ 0 \\ 0 \end{bmatrix}, \begin{bmatrix} 0 \\ 1 \\ 0 \\ 0 \end{bmatrix}, \begin{bmatrix} 0 \\ 0 \\ 1 \\ 0 \end{bmatrix}, \begin{bmatrix} 0 \\ 0 \\ 0 \\ 1 \end{bmatrix} \right\}, \quad (36)$$

assuming that there are K intervals over which the thrust is constant.

The middle time of the thrust $t_{i,j}$ and the half width durations of the thrusts $\Delta t_{i,j}$ are ranked in the increasing thrust middle times order t_1, \dots, t_P , assuming that there are P thrusts, and transformed to the commutation times as:

$$\begin{cases} s_{2k-1} = t_k - \Delta t_k, \\ s_{2k} = t_k + \Delta t_k, \end{cases}, k = 1, \dots, P. \quad (37)$$

In this case, the following equality holds : $K = 2P + 1$.

In order to guarantee both the operationally and the SK-feasibility of the state trajectory, a step (C) relying on the switched systems theory with the results of step (B) as initialization is used to enforce all the constraints while reducing the consumption.

5. Optimization of the Commutation Times with the Switched Systems Theory (step (C))

The reference [35] presents a technique to optimize the commutation times between the different subsystems. This method resorts to a time change of coordinates and a parametrization of the commutation times. The control profile computed at the end of the step (B) is an on-off control profile. The idea of this step is to notice that a bang-bang profile is a sequence of commutations between a system for which the control is on and another system for which the control is off. Hence, the date when the thruster switches on or switches off can be seen as a commutation between the subsystem for which the control is on to the subsystem for which the control is off, or vice-versa. This remark applies to the four thrusters of the considered satellite. Hence the method proposed by [35] will be applied in order to optimize the commutations between the coasting and the firing arcs. To this end, it is mandatory to assume that the order of the sequence of the active subsystems is an operationally feasible one. As the control profile computed at the end of step (B) is operationally feasible, this firing sequence can be used. Seeking these on and off times is equivalent to find the optimal commutation times between the subsystems.

Noting that each firing arc is separated by a coasting arc, the odd commutation times thus correspond to the beginning of a thrust and the even ones to the ending of a thrust. The notation of the commutation times is extended to $s_0 = t_0$ and $s_{2P+1} = t_f$. Therefore, minimizing the fuel consumption is equivalent to minimize the length of the intervals on which the thrusters are on. Hence the objective function is written as:

$$J_C(\{s_k\}) = F_{max} \sum_{i=1}^P (s_{2i} - s_{2i-1}). \quad (38)$$

The state constraints are handled by mean of the penalization term described by Equation (22) added to the

objective function. The new objective function for the step (C) of the decomposition method reads thus:

$$\begin{aligned} \tilde{J}_C(x, \{s_k\}) = & F_{max} \sum_{i=1}^P (s_{2i} - s_{2i-1}) \\ & + \mu_3 \sum_{k=1}^{2P+1} (s_k - s_{k-1}) \int_{k-1}^k \psi(t(\tau), x) d\tau, \end{aligned} \quad (39)$$

with μ_3 a parameter that balance the objective function between the fuel consumption minimization and the stay in the SK window. Note that μ_3 may be different from μ_1 defined in Equation (24). The tuning of this parameter may be a difficult issue to settle since selecting μ_3 too large results in an overconsumption while a too small μ_3 leads to an infeasible trajectory.

As in the reference [35], the time change of coordinates is used to parametrize the switching times:

$$t = s_k + \Delta_k(\tau - k) \quad \text{if } t \in [s_k, s_{k+1}], \quad (40)$$

with $\Delta_k = s_{k+1} - s_k$. The system dynamics is rewritten with the new time variable:

$$\frac{dx(\tau)}{d\tau} = \begin{cases} \Delta_{2k-2} \left[A(t(\tau))x(\tau) + D(t(\tau)) \right] & \text{if } \tau \in [2k-2, 2k-1], \\ \Delta_{2k-1} \left[A(t(\tau))x(\tau) + D(t(\tau)) + B(t(\tau))\Gamma F_{max} U_k \right] & \text{if } \tau \in [2k-1, 2k], \\ \vdots \\ \Delta_{2P} \left[A(t(\tau))x(\tau) + D(t(\tau)) \right] & \text{if } \tau \in [2P, 2P+1], \end{cases} \quad (41)$$

for $k = 1, \dots, P$. The state vector can now be considered as a function of the new time variable τ and of the switching times s_k : $x = x(\tau, \{s_k\})$.

The station keeping OCP reads thus in the switching systems framework:

Problem 6. Find the optimal, switching sequence $\{s_k\}$, $k \in \{1, \dots, 2P\}$, with P fixed, solution of the min-

imization problem:

$$\begin{aligned} \min_{x, \{s_k\}} J_C(x, \{s_k\}) = & F_{max} \sum_{i=1}^P (s_{2i} - s_{2i-1}) \\ & + \mu_3 \sum_{k=1}^{2P+1} (s_k - s_{k-1}) \int_{k-1}^k \psi(t(\tau), x) d\tau, \\ \text{s. t.} & \\ \dot{x}(\tau) = & \begin{cases} \Delta_{2k-2} \left[A(t(\tau))x(\tau) + D(t(\tau)) \right] & \text{if } \tau \in [2k-2, 2k-1], \\ \Delta_{2k-1} \left[A(t(\tau))x(\tau) + D(t(\tau)) + B(t(\tau))\Gamma F_{max} U_k \right] & \text{if } \tau \in [2k-1, 2k] \end{cases} \\ x(0) = & 0, \\ s_{2k} - s_{2k-1} \geq & T_l, \\ s_{2k+1} - s_{2k} \geq & T_g, \end{aligned} \quad (42)$$

with $T_g = T_s$ for the firing arcs of the same thruster and $T_g = T_d$ for the firing arcs of two different thrusters. \circ

As the switching times determine the structure of the control profile, the state trajectory is recovered by propagation of the system dynamics from the initial condition.

Problem 6 can be solved with a descent algorithm. To this end, it is necessary to compute the derivative of the performance index in order to obtain the descent direction. The computation of this derivative requires to distinguish the odd and the even commutation times:

$$\begin{aligned} \frac{dJ_C}{ds_{2l-1}} = & -F_{max} \\ & + \mu_3 \int_{2l-2}^{2l-1} \psi(t(\tau), x(\tau)) d\tau - \mu_3 \int_{2l-1}^{2l} \psi(t(\tau), x(\tau)) d\tau \\ & + \mu_3 (s_{2l-1} - s_{2l-2}) \int_{2l-2}^{2l-1} \left[(\tau - 2l + 2) \frac{\partial \psi}{\partial t}(t(\tau), x(\tau)) \right. \\ & \left. + \frac{\partial \psi}{\partial x}(t(\tau), x(\tau)) \frac{\partial x}{\partial s_{2l-1}}(\tau) \right] d\tau \\ & + \mu_3 (s_{2l} - s_{2l-1}) \int_{2l-1}^{2l} \left[(-\tau + 2l + 2) \frac{\partial \psi}{\partial t}(t(\tau), x(\tau)) \right. \\ & \left. + \frac{\partial \psi}{\partial x}(t(\tau), x(\tau)) \frac{\partial x}{\partial s_{2l-1}}(\tau) \right] d\tau, \end{aligned} \quad (43)$$

and :

$$\begin{aligned}
\frac{dJ_C}{ds_{2l}} &= F_{max} \\
&- \mu_3 \int_{2l}^{2l+1} \psi(t(\tau), x(\tau)) d\tau + \mu_3 \int_{2l-1}^{2l} \psi(t(\tau), x(\tau)) d\tau \\
&+ \mu_3 (s_{2l+1} - s_{2l}) \int_{2l}^{2l+1} \left[(-\tau + 2l + 1) \frac{\partial \psi}{\partial t}(t(\tau), x(\tau)) \right. \\
&\quad \left. + \frac{\partial \psi}{\partial x}(t(\tau), x(\tau)) \frac{\partial x}{\partial s_{2l-1}}(\tau) \right] d\tau \\
&+ \mu_3 (s_{2l} - s_{2l-1}) \int_{2l-1}^{2l} \left[(\tau - 2l + 1) \frac{\partial \psi}{\partial t}(t(\tau), x(\tau)) \right. \\
&\quad \left. + \frac{\partial \psi}{\partial x}(t(\tau), x(\tau)) \frac{\partial x}{\partial s_{2l-1}}(\tau) \right] d\tau.
\end{aligned} \tag{44}$$

As the switching times $\{s_k\}$ are independent of the time variable τ , the derivatives of the state vector with respect to the commutation times verify the following relation:

$$\frac{d}{d\tau} \left(\frac{\partial x(\tau)}{\partial s_k} \right) = \frac{\partial}{\partial s_k} \left(\frac{dx(\tau)}{d\tau} \right). \tag{45}$$

It is thus possible to derive a dynamic equation for $\frac{\partial x(\tau)}{\partial t_k}$ by differentiation of the dynamics equation of the state vector $x(\tau)$ with respect to the commutation time s_k . Hence the function $\tau \mapsto \frac{\partial x(\tau)}{\partial s_k}$ is obtained by integrating the following dynamics equations:

$$\frac{d}{d\tau} \left(\frac{\partial x(\tau)}{\partial s_{2l-1}} \right) = \left\{ \begin{array}{l} \bullet (s_{2k-1} - s_{2k-2}) A(t(\tau)) \frac{\partial x(\tau)}{\partial s_{2l-1}} \\ \quad \text{if } \tau \in [2k-2, 2k-1], k \neq l, \\ \bullet (s_{2k} - s_{2k-1}) A(t(\tau)) \frac{\partial x(\tau)}{\partial s_{2l-1}} \\ \quad \text{if } \tau \in [2k-1, 2k], k \neq l, \\ \bullet A(t(\tau)) x(\tau) + D(t(\tau)) \\ \quad + (s_{2l-1} - s_{2l-2}) \left[(\tau - 2l + 2) \left(\frac{\partial A(t)}{\partial t} x(\tau) + \right. \right. \\ \quad \left. \left. \frac{\partial D(t)}{\partial t} \right) + A(t(\tau)) \frac{\partial x(\tau)}{\partial s_{2l-1}} \right] \\ \quad \text{if } \tau \in [2l-2, 2l-1], \\ \bullet - \left[A(t(\tau)) x(\tau) + D(t(\tau)) + B(t(\tau)) U_l \right] \\ \quad + (s_{2l} - s_{2l-1}) \left[(-\tau + 2l + 2) \left(\frac{\partial A(t)}{\partial t} x(\tau) \right. \right. \\ \quad \left. \left. + \frac{\partial D(t)}{\partial t} + \frac{\partial B(t)}{\partial t} U_l \right) + A(t(\tau)) \frac{\partial x(\tau)}{\partial s_{2l-1}} \right] \\ \quad \text{if } \tau \in [2l-1, 2l], \end{array} \right. \tag{46}$$

and

$$\frac{d}{d\tau} \left(\frac{\partial x(\tau)}{\partial s_{2l}} \right) = \left\{ \begin{array}{l} \bullet (s_{2k-1} - s_{2k-2}) A(t(\tau)) \frac{\partial x(\tau)}{\partial s_{2l}} \\ \quad \text{if } \tau \in [2k-2, 2k-1], k \neq l, \\ \bullet (s_{2k} - s_{2k-1}) A(t(\tau)) \frac{\partial x(\tau)}{\partial s_{2l}} \\ \quad \text{if } \tau \in [2k-1, 2k], k \neq l, \\ \bullet - \left[A(t(\tau)) x(\tau) + D(t(\tau)) \right] \\ \quad + (s_{2l+1} - s_{2l}) \left[(-\tau + 2l + 1) \left(\frac{\partial A(t)}{\partial t} x(\tau) + \right. \right. \\ \quad \left. \left. \frac{\partial D(t)}{\partial t} \right) + A(t(\tau)) \frac{\partial x(\tau)}{\partial s_{2l}} \right] \\ \quad \text{if } \tau \in [2l, 2l+1], \\ \bullet A(t(\tau)) x(\tau) + D(t(\tau)) + B(t(\tau)) U_l \\ \quad + (s_{2l} - s_{2l-1}) \left[(\tau - 2l + 1) \left(\frac{\partial A(t)}{\partial t} x(\tau) \right. \right. \\ \quad \left. \left. + \frac{\partial D(t)}{\partial t} + \frac{\partial B(t)}{\partial t} U_l \right) + A(t(\tau)) \frac{\partial x(\tau)}{\partial s_{2l}} \right] \\ \quad \text{if } \tau \in [2l-1, 2l]. \end{array} \right. \tag{47}$$

The derivative of the penalization function with respect

to the state vector is:

$$\begin{aligned} \frac{\partial \psi}{\partial x}(t, x(\tau)) = & \\ & 2C_2(t) [C_2(t)x(t) - \delta] [\text{sign}(C_2(t)x(t) - \delta) + 1] \\ & + 2C_2(t) [C_2(t)x(t) + \delta] [\text{sign}(-C_2(t)x(t) - \delta) + 1] \\ & + 2C_3(t) [C_3(t)x(t) - \delta] [\text{sign}(C_3(t)x(t) - \delta) + 1] \\ & + 2C_3(t) [C_3(t)x(t) + \delta] [\text{sign}(-C_3(t)x(t) - \delta) + 1], \end{aligned} \quad (48)$$

and its derivative with respect to time is:

$$\begin{aligned} \frac{\partial \psi}{\partial t}(t, x(\tau)) = & \\ & 2 \frac{dC_2(t)}{dt} x [C_2(t)x(t) - \delta] [\text{sign}(C_2(t)x(t) - \delta) + 1] \\ & + 2 \frac{dC_2(t)}{dt} x [C_2(t)x(t) + \delta] [\text{sign}(-C_2(t)x(t) - \delta) + 1] \\ & + 2 \frac{dC_3(t)}{dt} x [C_3(t)x(t) - \delta] [\text{sign}(C_3(t)x(t) - \delta) + 1] \\ & + 2 \frac{dC_3(t)}{dt} x [C_3(t)x(t) + \delta] [\text{sign}(-C_3(t)x(t) - \delta) + 1]. \end{aligned} \quad (49)$$

The ensuing nonlinear non convex optimization problem is solved by an interior point algorithm based on [47] and encapsulated in the function `fmincon` in MATLAB®.

Putting all the three steps (A), (B) and (C) together, the SK problem can therefore be solved according to Algorithm 1.

6. Numerical Results

The proposed three-step decomposition method is applied on a realistic example and its benefit on the reduction of the fuel consumption while enforcing both the operational and SK constraints is demonstrated.

The considered satellite weights 4850 kg and is equipped with the 4 electric thrusters propulsion system described in Section 2.2 with thrusters in the North-East, North-West, South-East and South-West directions. This satellite has to be controlled in order to remain close to its geostationary position at a fixed longitude λ_{sk} and a fixed latitude $\varphi_{sk} = 0$. The station keeping is performed over the time horizon defined by $t_0 = 0$ and $t_f = 1$ week using the three-step technique described in this paper.

6.1. Solution of step (A)

The slope parameter M for the approximated switching function is arbitrarily chosen to be increased from 10^0 to 10^4 and from trial and error numerical simulations, it appears that the best choice for the tuning parameter μ_1 is $\mu_1 = 1.10^4$. On the Figure 6 depicting the continuous control profile, it is possible to notice that the operational constraints are not respected, as the thrusters 1 and 3 have simultaneous firings as well as the thrusters 2 and 4. Therefore, the step (A) is not sufficient to solve the whole

Algorithm 1 Solve the minimum fuel SK problem

Require: $x(t_0)$ the initial position

Ensure: the trajectory is operationally and SK-feasible

{Step (A): SK problem without the operational constraints}

- 1: Remove the operational constraints (i)-(iv) from Problem 1
- 2: $\tilde{F}_i(t)_{i=1,\dots,4,t \in [t_0, t_f]} \leftarrow$ the optimal control for the SK-feasible trajectory computed by an indirect method initialized by a direct method (see the reference [33])
- 3: $\varsigma \leftarrow$ threshold parameter to transform the continuous control profile in a rectangle profile
- 4: $\{t_{i,k}, \Delta t_{i,k}, \{U_k\}\} \leftarrow$ the middle times $t_{i,k}$ and the half durations $\Delta t_{i,k}$ of the thrusts,

{Step (B): equivalence schemes}

- 5: $\{t_{i,k}^*, \Delta t_{i,k}^*\} \leftarrow$ the middle times and half durations computed by the CBE or the EBE.

{Step (C): commutation times optimization with the switching systems technique}

- 6: $\{s_k\} \leftarrow$ the commutation times computed from $\{t_{i,k}^*, \Delta t_{i,k}^*\}$
 - 7: $\{s_k^{(0)}\} \leftarrow \{s_k\}$
 - 8: $\{s_k^*\} \leftarrow$ the solution of Problem 6 with an interior point algorithm
-

station keeping problem. The Table 1 shows that these two different values of the threshold parameter lead to different number of thrusts per thrusters. The two considered threshold parameters are $\varsigma_a = [0.8 \ 0.8 \ 0.8 \ 0.8]^T$ and $\varsigma_b = [0.9 \ 0.9 \ 0.9 \ 0.9]^T$. The threshold values depend on the configuration of the satellite and on the mission characteristics. Finely tuning these parameters is pivotal as the number of thrusts will remain fixed for the steps (B) and (C). In this study, these proposed values have been evaluated by proceeding a linear search.

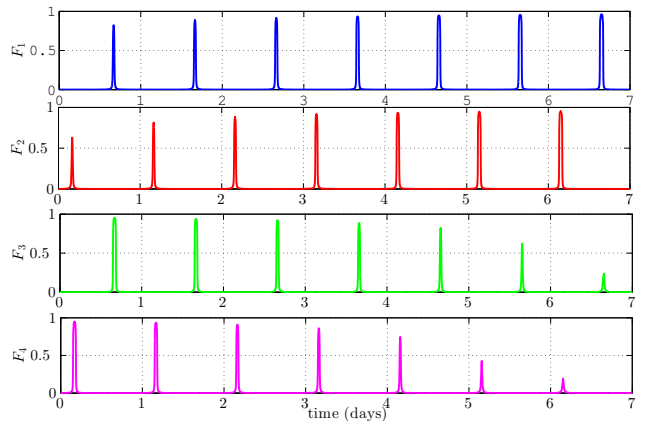


Figure 6: Continuous control profile at the end of step (A).

| Thruster | Threshold | |
|----------|---------------|---------------|
| | ς_a | ς_b |
| 1 | 7 | 5 |
| 2 | 6 | 4 |
| 3 | 5 | 3 |
| 4 | 4 | 3 |

Table 1: Number of thrusts per thrusters for the extracted on-off control profile at the end of step (A) with two values of the threshold parameter, ς_a and ς_b .

It is possible to find in the literature some rules of thumb for geostationary SK strategies, in particular in [1], [2] and [3]. In these references, the effect of the perturbing forces on the orbit is studied, and some general SK laws are derived. The North-South effect of the Sun and the Moon attractions are the most pregnant forces that must be corrected each half-orbit, once in the North direction and half an orbit later in the South direction. The East-West drift is meanwhile corrected by setting different thrust durations for each thrusters. This SK strategy was successfully used in an industrial context in [16]. The control profile of Figure 6 shows that the two South thrusters (F_2, F_4) have a thrust at the beginning of each day, and the two North thrusters (F_1, F_3) have a thrust half a day later. On the control profile, the thrusts have always different durations in order to compensate for the East-West drift. The physical rule of thumb can thus be recovered from a systematic optimization process.

6.2. Solution of step (B)

The trajectory obtained at the end of step (A) is SK-feasible but not operationally feasible. Therefore, the step (B) is mandatory in order to enforce the operational constraints. As described in the Section 4, the recovery of the middle time of the thrust and their half duration are very sensitive to the threshold parameter ς . Examples are given and some of them exhibit an operationally feasible but not SK-feasible state trajectory, depending of the value of ς . For ς_a , the trajectory computed after the CBE and EBE schemes are operationally feasible but not SK feasible (see Figure 7). Figure 8 displays the state trajectory computed with the CBE scheme and $\varsigma_c = [0.89 \ 0.89 \ 0.93 \ 0.93]^T$ and the state trajectory computed with the EBE scheme and $\varsigma_d = [0.95 \ 0.9 \ 0.95 \ 0.95]^T$. In these two cases, a fine tuning of the threshold parameter leads to operationally and SK-feasible trajectory.

Despite the fact that some of the trajectories are not SK-feasible, the aim of this step is just to enforce the operational constraints since an operationally feasible initial solution is mandatory for the step (C), whose aim is to enforce the SK constraints.

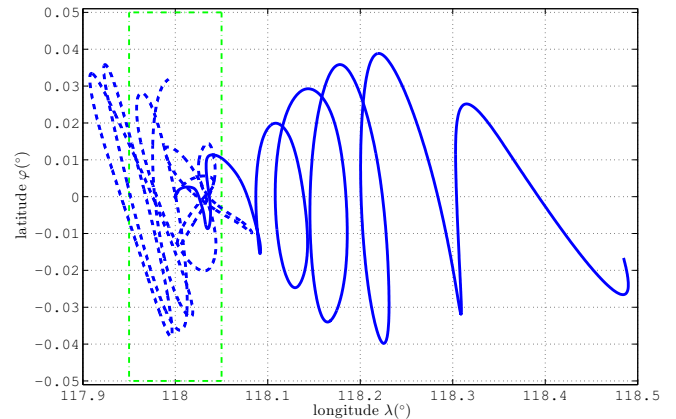


Figure 7: Trajectories in the (λ, φ) plane after the step (B).
— : CBE scheme with ς_a , - - : EBE scheme with ς_a ,
- - - : station keeping window.

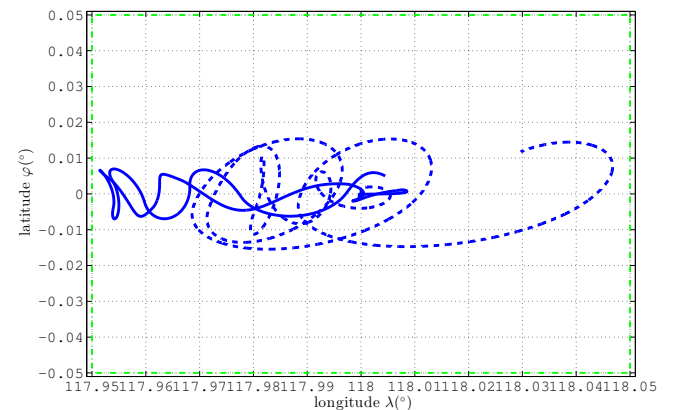


Figure 8: Trajectories in the (λ, φ) plane after the step (B).
— : CBE scheme with ς_c , - - : EBE scheme with ς_d ,
- - - : station keeping window.

6.3. Solution of step (C)

The step (C) optimizes the commutation times of the control profile solution of step (B). The firing sequence from the step (B) is supposed to be the optimal one, and its commutation times have to be optimized. For both equivalence schemes of the step (B), this step manages to minimize the fuel consumption while enforcing the operational as well as the SK constraints. For the two state trajectories of Figure 8 computed with ς_c and ς_d , the step (C) reduces the fuel consumption, as the Table 2 shows. Figures 9 and 10 display the control profile optimized thanks to the switching system framework. On these Figures, it appears that the length of the thrusts have been reduced, implying a decrease of the consumption. Figures 11 and 12 illustrate the fact that even if the trajectory resulting from step (B) is not SK-feasible, the optimization of the commutation times performed in step (C) manages to enforce the SK constraints, The Figures 13 and 14 show that this step reduces the consumption as well.

For these computations, $\mu_3 = 10^8$. As the integration of

the dynamics equation (41) and its time derivatives with respect to the switching times (46) and (47) are numerically integrated with large steps in order to reduce the computation time, some margins have been taken and the size of the SK window has been reduced by 10%.

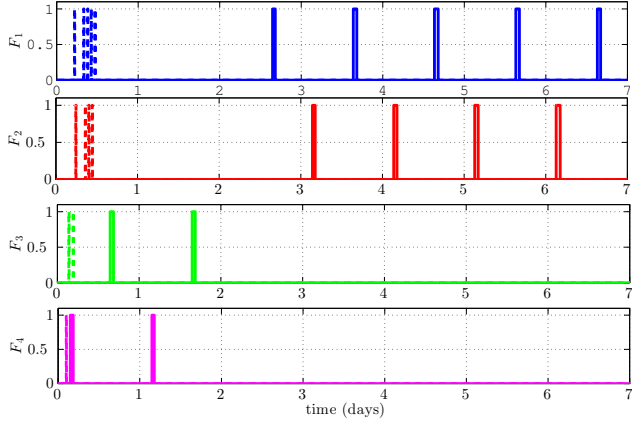


Figure 9: Control profiles :
— : after the step (B) with ς_c and the CBE scheme (total thrust duration: 24.35 hours),
- - : after step (C) (total thrust duration: 72.43 min).

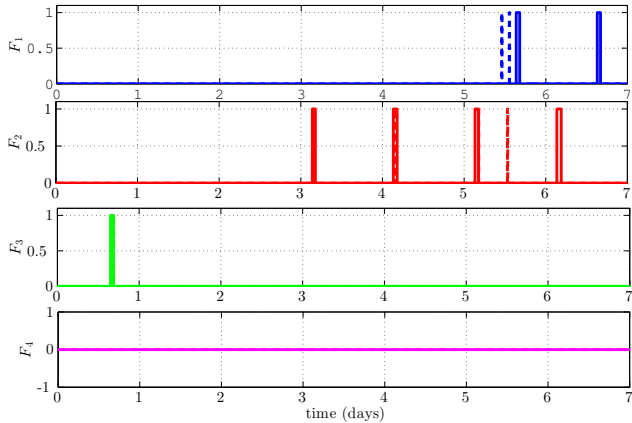


Figure 10: Control profiles :
— : after the step (B) with ς_d and the EBE scheme (total thrust duration: 7.17 hours),
- - : after step (C) (total thrust duration: 26.78 min).

In Table 2, several values of the threshold parameter ς used at the end of the step (A) are given, as well as the stemmed number of thrusts P . This Table 2 shows clearly the fuel consumption reduction between the steps (B) and (C).

In the reference [13], the SK strategy leads to a velocity increment budget of 3.204 m/s for 10 days, which leads to 2.24 m/s for a week. In [2, Table 3, p.150], it is possible to find inclination correction requirements for one year. According to the authors strategy, the annual velocity correction to be performed is a least 78.67 m/s, i.e. 1.51 m/s for a week. Therefore, the proposed three-step correction

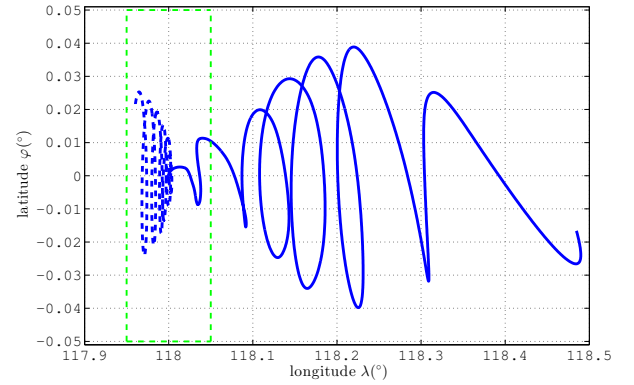


Figure 11: Trajectories in the (λ, φ) plane :
— : after the step (B) with ς_a and the CBE scheme,
- - : after step (C),
- - : station keeping window.

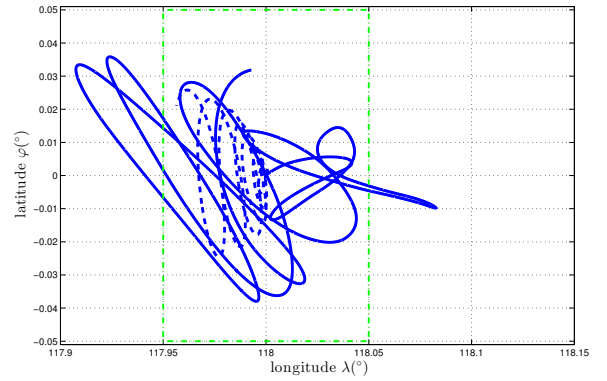


Figure 12: Trajectories in the (λ, φ) plane :
— : after the step (B) with ς_a and the EBE scheme,
- - : after step (C),
- - : station keeping window.

algorithm creates SK strategies that require less fuel consumption than the ones existing in the litterature.

7. Conclusion

In this paper, a decomposition of the overall station keeping optimal control problem under many operational constraints is used to take into account some difficult constraints inherent to the use of electric propulsion. In a first step, a classical optimal control problem is solved with state constraints using a precise indirect method initialized by a collocation based direct method. In a second step, two ways of dealing with the thrusters operational constraints are proposed resulting in two different fuel consumption results. In a third step, an optimization of the commutation times coming from the theory of the switched systems is used in order to optimize the on and off times of the firing sequence obtained at the end of the second step. In fact, the system can be naturally decomposed into several subsystems, one per thruster whose control is on and

| Threshold $\begin{bmatrix} \zeta_1 & \zeta_2 & \zeta_3 & \zeta_4 \end{bmatrix}^T$ | P | Equivalence scheme | Consumption for step (B) | SK performed | Consumption for step (C) | SK performed |
|--|-----|-----------------------|-----------------------------|-----------------|-----------------------------|-----------------|
| $\begin{bmatrix} 0.89 & 0.89 & 0.93 & 0.93 \end{bmatrix}^T$ | 13 | CBE | 3.51 m/s | yes | 0.31 m/s | yes |
| $\begin{bmatrix} 0.89 & 0.88 & 0.93 & 0.93 \end{bmatrix}^T$ | 14 | CBE | 4.41 m/s | yes | 0.33 m/s | yes |
| $\begin{bmatrix} 0.9 & 0.9 & 0.95 & 0.95 \end{bmatrix}^T$ | 10 | EBE | 1.65 m/s | yes | 0.24 m/s | yes |
| $\begin{bmatrix} 0.95 & 0.9 & 0.95 & 0.95 \end{bmatrix}^T$ | 7 | EBE | 2.05 m/s | yes | 0.17 m/s | yes |
| $\begin{bmatrix} 0.8 & 0.8 & 0.8 & 0.8 \end{bmatrix}^T$ | 22 | CBE | 21.45 m/s | no | 0.52 m/s | yes |
| $\begin{bmatrix} 0.8 & 0.8 & 0.8 & 0.8 \end{bmatrix}^T$ | 22 | EBE | 22.52 m/s | no | 0.52 m/s | yes |

Table 2: Consumptions at the end of steps (B) and (C) with respect to the chosen threshold parameter ζ at the end of step (A).

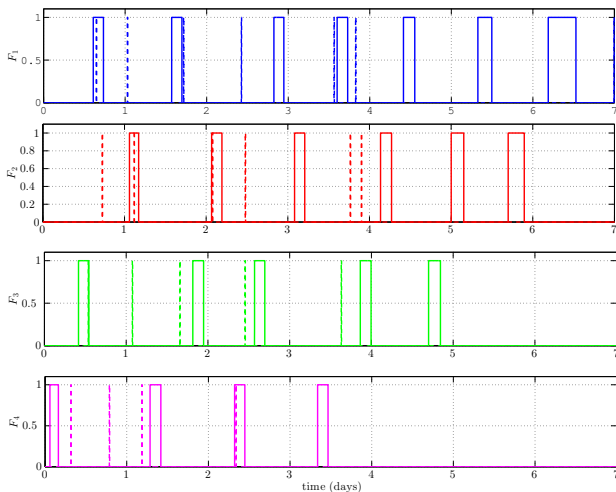


Figure 13: Control profiles :
— : after the step (B) with ζ_a and the CBE scheme,
- - : after step (C).

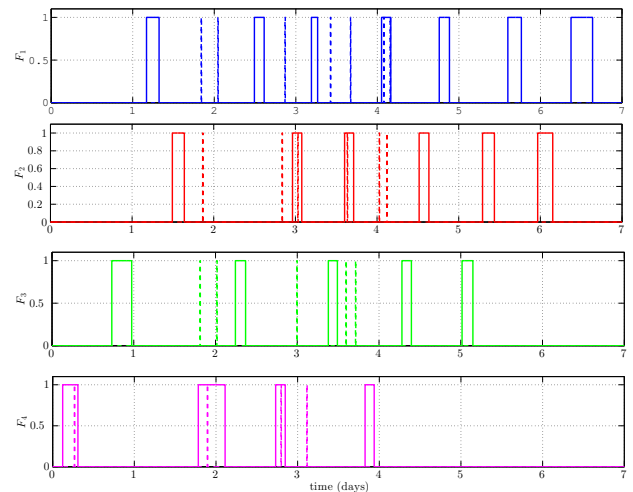


Figure 14: Control profiles :
— : after the step (B) with ζ_a and the EBE scheme,
- - : after step (C).

one corresponding to a coasting arc. As demonstrated by the numerical examples, the threshold parameter used in the first step has a high impact on the control profile computed at the second step, so that the resulting trajectory may not be SK-feasible in some cases. However, as this trajectory is operationally feasible, the third step objective is to enforce both the operational and the SK constraints. Despite these positive results, some issues remain open. The state constraints are taken into account with a penalization function, but alternative formulations of the first order necessary conditions coming from the Pontryagin Maximum Principle exist and should be considered. Furthermore, in the last step, the dynamics and its time derivative have to be numerically integrated, once per commutation time. This leads to long resolution time, that could be lowered using semi-analytic integration tools for instance.

References

- [1] G. Campan, F. Alby, H. Gautier, Les techniques de maintien à poste de satellites géostationnaires, in: *Mécanique Spatiale*, cnes Edition, Cépaduès-Editions, Toulouse, France, 1995, Ch. 15, pp. 983–1085.
- [2] E. M. Soop, *Handbook of Geostationary Orbits*, Kluwer Academic Publishers Group, 1994.
- [3] M. J. Sidi, *Spacecraft Dynamics and Control*, Cambridge University Press, 1997.
- [4] C. Chao, H. Bernstein, Onboard stationkeeping of geosynchronous satellite using a global positioning system receiver, *Journal of Guidance, Control, and Dynamics* 17 (4) (1994) 778–786. doi:10.2514/3.21267.
- [5] T. S. No, Simple Approach to East-West Station Keeping of Geosynchronous Spacecraft, *Journal of Guidance Control and Dynamics* 22 (5) (1999) 734–736.
- [6] B. P. Emma, H. J. Pernicka, Algorithm for Autonomous Longitude and Eccentricity Control for Geostationary Spacecraft, *Journal of Guidance, Control, and Dynamics* 26 (3) (2003) 483–490. doi:10.2514/2.5071. URL <http://arc.aiaa.org/doi/abs/10.2514/2.5071>
- [7] B. K. Park, M. J. Tahk, H. C. Bang, C. S. Park, J. H.

- Jin, A new approach to on-board stationkeeping of GEO-satellites, *Aerospace Science and Technology* 9 (8) (2005) 722–731. doi:10.1016/j.ast.2005.08.004.
- [8] V. M. Gomes, A. F. B. a. Prado, Low-thrust out-of-plane orbital station-keeping maneuvers for satellites, *Mathematical Problems in Engineering* doi:10.1155/2012/532708.
- [9] R. Boucher, Electric Propulsion for Control of Stationary Satellites, in: *AIAA Electric Propulsion Conference*, no. 1, Colorado Springs, Colorado, 1963.
- [10] J. H. Molitor, Ion Propulsion System for Stationary-Satellite Control, *Journal of Spacecraft and Rockets* 1 (2) (1964) 170–175.
- [11] C. C. Barrett, On the Application of electric Propulsion to Satellite Orbit Adjustment and Station Keeping, in: *American Institute of Aeronautics and Astronautics, Electric propulsion and Plasmadynamics Conference*, Colorado Springs, Colorado, 1967. arXiv:arXiv:1011.1669v3, doi:10.1017/CBO9781107415324.004.
- [12] R. R. Hunziker, Low-Thrust Station Keeping Guidance for a 24-Hour Satellite, *AIAA Journal* 8 (7) (1970) 1186–1192.
- [13] M. C. Eckstein, Optimal Station Keeping by Electric Propulsion With Thrust Operation Constraints, *Celestial Mechanics* 21 (1978) 129–147.
- [14] M. C. Eckstein, F. Hechler, Station acquisition and Station-Keeping with Low Thrust Systems, in: *International Symposium Spacecraft Flight Dynamics*, Darmstadt, Germany, 1981.
- [15] M. C. Eckstein, A. Leibold, F. Hechler, Optimal autonomous station keeping of geostationary satellites, in: *AAS/AIAA Astrodynamics Specialist Conference*, 1981.
- [16] B. M. Anzel, Method and apparatus for a Satellite Station Keeping, US Patent 5,443,231 (August 1995).
- [17] N. S. Gopinath, K. N. Srinivasamuthy, Optimal low thrust orbit transfer from gto to geosynchronous orbit and stationkeeping using electric propulsion system, in: *54th International Astronautical Congress of the International Astronautical Federation, the International Academy of Astronautics, and the International Institute of Space Law*, no. October, Bremen, Germany, 2003, pp. 1–9.
- [18] D. Losa, M. Lovera, R. Draï, T. Dargent, J. Amalric, Electric Station Keeping of Geostationary Satellites: a Differential Inclusion Approach, *Proceedings of the 44th IEEE Conference on Decision and Control* (2005) 7484–7489 doi:10.1109/CDC.2005.1583369.
- [19] D. Losa, M. Lovera, J.-P. Marmorat, T. Dargent, J. Amalric, Station Keeping of Geostationary Satellites with On-Off Electric Thrusters, *Computer Aided Control System Design*, 2006 IEEE International Conference on Control Applications, 2006 IEEE International Symposium on Intelligent Control, 2006 IEEE (2006) 2890–2895 doi:10.1109/CCA.2006.286049.
- [20] A. Walsh, S. Di Cairano, A. Weiss, MPC for Coupled Station Keeping, Attitude Control, and Momentum Management of Low-Thrust Geostationary Satellites, in: *American Control Conference*, Boston, Massachusetts, USA, 2016, pp. 7408–7413. doi:10.1109/ACC.2016.7526842.
- [21] M. Peukert, B. Wollenhaupt, OHB-System’s View on Electric Propulsion Needs, in: *EPIC Workshop*, Brussels, 2014.
- [22] A. Sukhanov, A. Prado, On one approach to the optimization of low-thrust station keeping manoeuvres, *Advances in Space Research* 50 (11) (2012) 1478–1488. doi:10.1016/j.asr.2012.07.028.
- [23] G. Elnagar, M. A. Kazemi, M. Razzaghi, The Pseudospectral Legendre Method for Discretizing Optimal Control Problem, *IEEE Transactions on Automatic Control* 40 (10) (1995) 1793–1796.
- [24] C. R. Hargraves, S. W. Paris, Direct Trajectory Optimization using nonlinear programming and collocation.pdf, *Journal of Guidance, Control, and Dynamics* 10 (4) (1987) 338–342.
- [25] D. G. Hull, Conversion of optimal control problems into parameter optimization problems, *Journal of Guidance, Control, and Dynamics* 20 (1) (1997) 57–60.
- [26] J. T. Betts, Survey of Numerical Methods for Trajectory Optimization, *Journal of Guidance, Control, and Dynamics* 21 (2) (1998) 193–207. doi:10.2514/2.4231.
- [27] J. T. Betts, W. P. Huffman, Mesh refinement in direct transcription methods for optimal control, *Optimal Control Applications and Methods* 19 (1) (1998) 1–21.
- [28] J. T. Betts, Very Low Thrust Trajectory Optimization Using a Direct SQP Method, *Journal of Computational and Applied Mathematics* 120 (2000) 27–40.
- [29] A. Weiss, S. Di Cairano, Opportunities and Potential of Model Predictive Control for Low-Thrust Spacecraft Station-Keeping and Momentum-Management, in: *European Control Conference*, Linz, Austria, 2015, pp. 1364–1369.
- [30] A. Weiss, U. Kalabic, S. Di Cairano, Model Predictive Control for Simultaneous Station Keeping and Momentum Management of Low-Thrust Satellites, *American Control Conference* (2015) 2305–2310.
- [31] R. Vazquez, F. Gavilan, E. F. Camacho, Trajectory Planning for Spacecraft Rendezvous in elliptical orbits with On / Off Thrusters, in: *19th IFAC World Congress*, Cap Town, South Africa, 2014, pp. 8473–8478.
- [32] R. Vazquez, F. Gavilan, E. F. Camacho, Pulse-Width Predictive Control for LTV Systems with Application to Spacecraft Rendezvous, arXiv preprint arXiv:1511.00869.
- [33] C. Gazzino, D. Arzelier, D. Losa, C. Louembet, C. Pittet, L. Cerri, Optimal Control for Minimum-Fuel Geostationary Station Keeping of Satellites Equipped with Electric Propulsion, in: *20th IFAC Symposium on Automatic Control in Aerospace - ACA 2016*, Sherbrooke, Canada, 2016.
- [34] C. Gazzino, D. Arzelier, L. Cerri, D. Losa, C. Louembet, C. Pittet, Solving the Minimum-Fuel Low-Thrust Geostationary Station Keeping Problem via the Switching Systems Theory, in: *European Conference for Aeronautics and AeroSpace Sciences*, Milan, Italy, 2017.
- [35] X. Xu, P. J. Antsaklis, Optimal control of switched systems based on parameterization of the switching instants, *IEEE Transactions on Automatic Control* 49 (1) (2004) 2–16. doi:10.1109/TAC.2003.821417.
- [36] R. H. Battin, *An Introduction to the Mathematics and Methods of Astrodynamics*, Education. AIAA., 1999. doi:10.2514/4.861543.
- [37] S. K. Shrivastava, Orbital Perturbations and Stationkeeping of Communication Satellites, *Journal of Spacecraft* 15 (2).
- [38] G. Campan, P. Brousse, ORANGE: Orbital analytical model for geosynchronous satellite, *Revista Brasileira de Ciências Mecânicas* 16 (16) (1994) 561–572.
- [39] W. Grimm, A. Markl, Adjoint estimation from a direct multiple shooting method, *Journal of optimization theory and applications* 92 (2) (1997) 263–283.
- [40] O. von Stryk, R. Bulirsch, Direct and indirect methods for trajectory optimization, *Annals of Operations Research* 37 (1) (1992) 357–373.
- [41] D. S. Naidu, *Optimal Control Systems*, crc press Edition, 2002.
- [42] B. Bonnard, L. Faubourg, E. Trélat, *Mécanique céleste et contrôle des véhicules spatiaux*, springer s Edition, 2005.
- [43] L. Mazal, G. Mingotti, P. Gurfil, Optimal On-Off Cooperative Maneuvers for Long-term Satellite Cluster Flight, *Journal of Guidance, Control, and Dynamics* 37 (2) (2014) 391–402.
- [44] R. Bulirsch, E. Nerz, H. J. Pesch, O. von Stryk, Combining direct and indirect methods in optimal control: Range maximization of a hang glider, *Optimal Control* (1993) 273–288.
- [45] B. Bonnard, L. Faubourg, G. Launay, E. Trélat, Optimal control with state constraints and the space shuttle re-entry problem, *Journal of Dynamics and Control Systems* 9 (2) (2003) 155–199.
- [46] P. J. Antsaklis, *Linear Systems*, Cambridge Aerospace Series, Birkhäuser, Boston, {M}assachusetts, {USA}, 2003.
- [47] R. Byrd, M. E. Hribar, J. Nocedal, An interior point algorithm for large-scale nonlinear programming, *SIAM Journal on Optimization* 9 (4) (1999) 877–900.